Cell PRESS
Structure
Short Article

The Three-Dimensional Structure of the Biotin Carboxylase-Biotin Carboxyl Carrier Protein Complex of *E. coli* Acetyl-CoA Carboxylase

Tyler C. Broussard,[1] Matthew J. Kobe,[1] Svetlana Pakhomova,[1] David B. Neau,[2] Amanda E. Price,[1] Tyler S. Champion,[1] and Grover L. Waldrop[1,*]
[1]Division of Biochemistry and Molecular Biology, Louisiana State University, Baton Rouge, LA 70803, USA
[2]Northeastern Collaborative Access Team, Argonne National Laboratory, Argonne, IL 60439, USA
*Correspondence: gwaldro@lsu.edu
http://dx.doi.org/10.1016/j.str.2013.02.001

SUMMARY

Acetyl-coenzyme A (acetyl-CoA) carboxylase is a biotin-dependent, multifunctional enzyme that catalyzes the regulated step in fatty acid synthesis. The *Escherichia coli* enzyme is composed of a homodimeric biotin carboxylase (BC), biotinylated biotin carboxyl carrier protein (BCCP), and an $\alpha_2\beta_2$ heterotetrameric carboxyltransferase. This enzyme complex catalyzes two half-reactions to form malonyl-coenzyme A. BC and BCCP participate in the first half-reaction, whereas carboxyltransferase and BCCP are involved in the second. Three-dimensional structures have been reported for the individual subunits; however, the structural basis for how BCCP reacts with the carboxylase or transferase is unknown. Therefore, we report here the crystal structure of *E. coli* BCCP complexed with BC to a resolution of 2.49 Å. The protein-protein complex shows a unique quaternary structure and two distinct interfaces for each BCCP monomer. These BCCP binding sites are unique compared to phylogenetically related biotin-dependent carboxylases and therefore provide novel targets for developing antibiotics against bacterial acetyl-CoA carboxylase.

INTRODUCTION

Biotin-dependent acetyl-coenzyme A carboxylase (ACC) catalyzes the regulated step in fatty acid synthesis in all domains of life. In *Escherichia coli*, ACC is made up of three components: biotin carboxylase (BC), biotin carboxyl carrier protein (BCCP), and carboxyltransferase (CT) (Cronan and Waldrop, 2002). The first step in the enzymatic reaction, catalyzed by BC, is the ATP-dependent carboxylation of the vitamin biotin (Figure 1), which is covalently attached to a specific lysine residue (Lys122) of BCCP. The second half-reaction carried out by CT is the transfer of the carboxyl group from the 1′N of carboxybiotin to acetyl-coenzyme A (acetyl-CoA) to form malonyl-CoA (Figure 1).

The genes encoding BC (Li and Cronan, 1992a) and CT (Li and Cronan, 1992b) have been cloned, overexpressed (Blanchard et al., 1999b; Blanchard and Waldrop, 1998), retain their enzymatic function in the absence of the other components, and utilize free biotin as a substrate instead of biotin linked to BCCP (Guchhait et al., 1974). The structure of *E. coli* BC has been determined in the absence of substrates (Thoden et al., 2000; Waldrop et al., 1994), with ATP analogs AMPPNP and ADPCF$_2$P (Mochalkin et al., 2008), and with biotin, bicarbonate, and Mg-ADP (Chou et al., 2009). The structure of CT has also been determined (Bilder et al., 2006). In addition, the structure of the C-terminal domain of BCCP, which contains the biotinylated lysine, has been determined by X-ray crystallography (Athappilly and Hendrickson, 1995) and nuclear magnetic resonance (NMR) (Yao et al., 1997). While the three-dimensional structures of the individual components have been of inestimable value, the fact remains that BCCP is the substrate for BC and CT, and therefore, what is lacking is a structure of either the biotin carboxyl carrier protein-biotin carboxylase (BCCP-BC) complex or the biotin carboxyl carrier protein-carboxyltransferase complex.

It was found that a stable BCCP-BC complex formed when purifying BCCP from an *E. coli* strain that coexpressed both proteins (Nenortas and Beckett, 1996), while Choi-Rhee and Cronan (2003) suggested that the stoichiometry of the protein complex was one BC homodimer bound to four BCCP molecules. Thus, since BC and BCCP form a complex, we undertook the determination of the crystal structure of that protein-protein interaction. Here, we report the three-dimensional structure of the *E. coli* BCCP-BC complex determined at 2.49 Å resolution. The structure indicates a stoichiometry different from that previously reported (Choi-Rhee and Cronan, 2003) and reveals a quaternary structure for BC that has heretofore never been observed.

RESULTS AND DISCUSSION

Copurification of BCCP and BC

The genes encoding BCCP (*accB*) and BC (*accC*) are located in an operon in the *E. coli* chromosome and are cotranscribed (James and Cronan, 2004). To mimic the in vivo arrangement, *accB* and *accC* were coexpressed using a minioperon where a histidine tag was put on the N terminus of BCCP. After purification by nickel affinity and size exclusion chromatography, the major peak contained the BCCP-BC complex, which was used for crystallization (Figure S1A available online). Gel

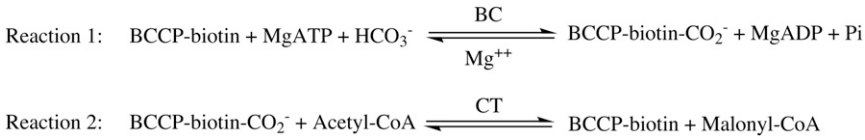

Figure 1. Reaction Catalyzed by Acetyl-CoA Carboxylase
Reaction 1 is catalyzed by biotin carboxylase and Reaction 2 is catalyzed by carboxyltransferase. Biotin is shown covalently attached to the biotin carboxyl carrier protein.

electrophoresis showed a band at 50 kDa corresponding to the BC monomer and a band at ~22 kDa that is indicative of full-length BCCP (Figure S1B). The BCCP runs slightly higher than its 16.7 kDa molecular weight; this is thought to be caused by a pro/ala-rich linker in the middle of the protein (Li and Cronan, 1992a). Most importantly, the fact that the BCCP-BC complex remains intact after both nickel affinity and size exclusion chromatography suggests that the BCCP-BC interaction is indeed stable.

Quaternary Structure

The overall structure of the BCCP-BC complex has D_2 symmetry and is shown in Figures 2A–2C. One of the most striking features of the BCCP-BC complex is that two BC homodimers (which have C2 symmetry) come together to form a tetramer. If the BC tetramer is viewed by looking at one homodimer on top of the other, then it becomes readily apparent that the homodimers are rotated approximately 90° with respect to one another (Figure 2C). Tetrameric BC in the BCCP-BC complex is in stark contrast to the structures reported to date of BC, which have shown the enzyme to be a homodimer with C2 symmetry (Chou et al., 2009; Mochalkin et al., 2008; Thoden et al., 2000; Waldrop et al., 1994). Moreover, there are no packing interfaces in the crystals of BC alone that display the same dimer-dimer interaction as the BCCP-BC complex.

The tetramer of BC is bound to four BCCP molecules where each BCCP molecule forms two interfaces. One interface is with a BC monomer located in the upper homodimer while the other is with a BC monomer in the lower homodimer of the tetramer (Figures 2A and 2B). Thus, the four BCCP molecules essentially act as molecular clips to hold two BC homodimers together to form a tetramer. It is important to note that the stoichiometry of two BC dimers plus four BCCP molecules observed here does not agree with the stoichiometry previously reported of one BC dimer and four BCCP molecules (Choi-Rhee and Cronan, 2003). Moreover, these investigators also concluded that the N-terminal domain of BCCP was required for the interaction of BCCP with BC (Choi-Rhee and Cronan, 2003). As can be seen in Figure 2D, it is the C-terminal region of BCCP that interacts with BC, which is consistent with kinetic studies showing the C-terminal domain is a substrate for BC (Blanchard et al., 1999a). Electron density for the N-terminal region was not observed, presumably due to inherent flexibility in this region of the molecule. Control experiments in which crystals of the BCCP-BC complex were run on SDS-PAGE show that the N-terminal domain is, in fact, attached to the C-terminal domain. The high degree of flexibility of the N-terminal domain of BCCP was also observed (by the lack of NOEs) in the N-terminal region of the 1.3S subunit of the homologous biotin-dependent enzyme transcarboxylase (Reddy et al., 1998). The N-terminal region of the 1.3S subunit is involved in contacts with the other subunits of transcarboxylase (Carey et al., 2004), and by inference the N-terminal domain of *E. coli* BCCP may also interact with the CT subunit of acetyl-CoA carboxylase. Moreover, the fact that the N-terminal domain of BCCP is not involved in binding to BC is consistent with the observations that this domain downregulates transcription of the *accBC* operon (James and Cronan, 2004). Thus, if BCCP and BC form a complex in vivo, then it is reasonable to assume that the N-terminal domain of BCCP must remain unhindered so it could bind DNA and act as a transcriptional repressor.

The quaternary structure shown here of two BC homodimers and four BCCP molecules has a molecular weight of ~260 kDa. However, the size exclusion chromatography data show a molecular weight greater than 640 kDa for the BCCP-BC complex (Figure S1A). Thus, the structure observed here is likely a monomer of a much larger complex. For instance, if the ~260 kDa BCCP-BC complex shown here were a trimer, then it would have a molecular weight of ~800 kDa, which would be consistent with the three-fold axis of symmetry observed in two other biotin-dependent enzymes, propionyl-CoA carboxylase (Huang et al., 2010) and methylcrotonyl-CoA carboxylase (Huang et al., 2012).

Several lines of evidence indicate that the BCCP-BC complex described here is physiologically relevant. First, the minioperon of BCCP-BC used in this study mirrors the operon and cotranscription of these two proteins that normally occurs in the cell. The reason that only a homodimer of biotin carboxylase has been crystallized before is because the gene for the enzyme was overexpressed in the absence of BCCP, which does not mimic the in vivo situation. Moreover, the homodimer of biotin carboxylase observed in previous crystal structures is part of the homotetramer observed here where the interaction of two homodimers forms a tetramer that is mediated by BCCP. Second, the formation of a BCCP-BC complex is also consistent with the observations that BCCP by itself forms aggregates (Choi-Rhee and Cronan, 2003; Nenortas and Beckett, 1996). Thus, formation of a complex between BCCP and BC is more likely to be the case in vivo rather than BC existing as a homodimer and BCCP as an aggregate. Third, the BCCP-BC complex presented here is unlikely to be a consequence of the crystallization conditions because the same structure was observed under different crystallization conditions and in a different crystal form, albeit at a lower resolution (3.7 Å) (Table 1; Supplemental Experimental Procedures).

BCCP Structure

The overall structure of the C-terminal domain of BCCP bound to BC is virtually identical to the crystal (Athappilly and Hendrickson, 1995) and NMR (Yao et al., 1997) structures of the C-terminal domain of BCCP. The root-mean-square deviations (rmsds) between the equivalent Cα atoms of BCCP molecule B in the BCCP-BC complex and the crystal and NMR structures

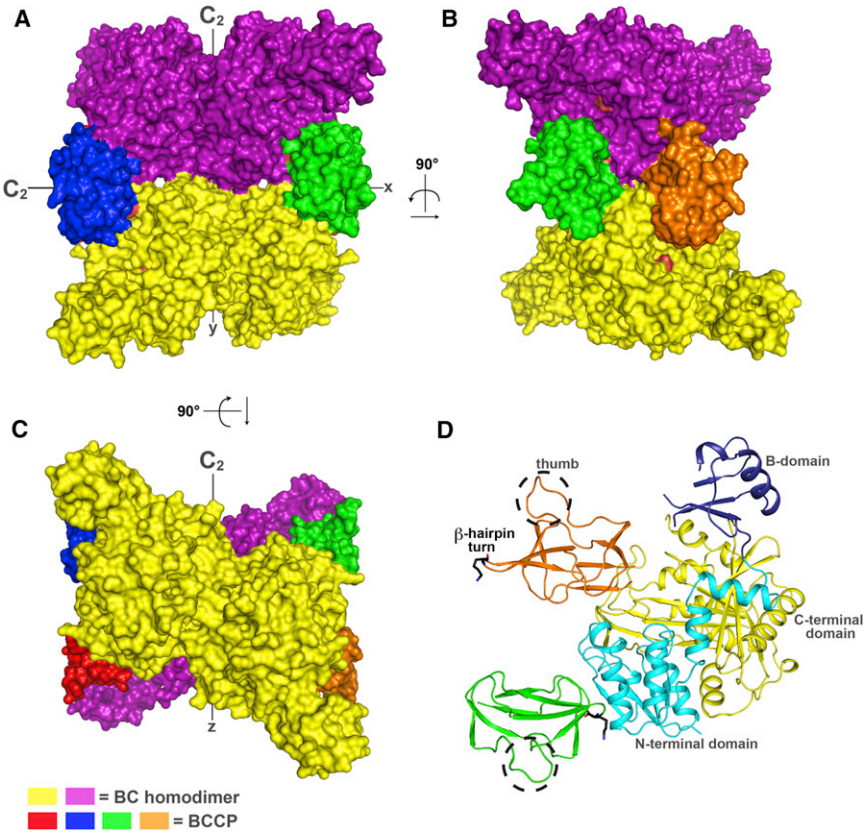

Figure 2. Quaternary Structure of the BCCP-BC Complex

(A–C) Surface rendering of the BCCP-BC complex showing the BC homodimer in purple (top) and yellow (bottom) with individual BCCPs shown in blue, green, orange, and red. (B) is (A) rotated 90° to the left and (C) is (A) rotated 90° around the x axis in a clockwise motion. The local symmetry axes of the BCCP-BC complex are also indicated in (A) and (C).

(D) Cartoon representation of a monomer of BC with the two interfacing BCCP molecules in orange and green, respectively. The N-terminal domain, B-domain, and the C-terminal domain of the BC monomer are labeled and colored in light blue, dark blue, and yellow, respectively. Lys122 is represented as black sticks in each BCCP molecule with oxygen and nitrogen atoms in red and blue, respectively. The thumb of each BCCP molecule is designated by dashed circles.

were 0.64 Å and 1.28 Å, respectively. When the *E. coli* BCCP molecules observed in the complex were superimposed to the Cα atoms of the BCCP domain from human ACC2 (Lee et al., 2008) and the 1.3S subunit of transcarboxylase from *Propionibacterium shermanii* (Reddy et al., 1998), the rmsds were 1.7 Å and 1.5 Å, respectively. Although the rmsds were calculated between the Cα atoms of matching residues, the major difference between these molecules is the lack of a "thumb" in the non-*E. coli* proteins (Figure 3). This "motif" is not involved in interacting with BC and extends out away from the main body of the BCCP-BC complex (Figure 2D). Mutations in this region of *E. coli* BCCP were found to impair the growth of *E. coli*, suggesting that it is important for the function of the protein; however, the chemical mechanism for this phenotype is not understood (Cronan, 2001).

The hairpin turn in BCCP that contains the lysine residue that is biotinylated also protrudes away from the main body of the BCCP-BC complex (Figure 2D). The Cα of Lys122 is ~40 Å from Arg338, which is an active site residue that is important for catalysis (Sloane and Waldrop, 2004). The Cα of Lys122 was used as a reference because no electron density for the side chain of this residue was observed. This distance is consistent with the structures of the related biotin-dependent holoenzymes propionyl-CoA carboxylase, pyruvate carboxylase, and methylcrotonyl-CoA carboxylase, which have distances between the BC and CT active sites of 55, 75, and 80 Å, respectively (Huang et al., 2010, 2012; Xiang and Tong, 2008). Considerable movement of the BCCP domain has been proposed for catalysis by other biotin-dependent carboxylases (Huang et al., 2012; St Maurice et al., 2007; Xiang and Tong, 2008) and BCCP has been observed in different positions in the cryo-electron microscopy studies on propionyl-CoA carboxylase (Huang et al., 2010). Thus, it is not surprising that the *E. coli* BCCP is ~40 Å away from the BC active site and may possibly be equidistant from where the BC and CT active sites would be in a full structure (~80 Å).

The large distance between biotinylated BCCP and the active site is also in accord with reports that the BCCP-BC complex exhibits little to no catalytic activity in the absence of CT (Alves et al., 2011; Soriano et al., 2006). Measurements of the enzymatic activity of the BCCP-BC complex used in this study confirm the previous studies in that the activity of the BCCP-BC complex was 0.005 μmol/min/mg, while the activity in the presence of CT and acetyl-CoA increased markedly (0.530 μmol/min/mg), suggesting that BCCP in the complex was at least partially biotinylated. Thus, the BCCP-BC complex is catalytically competent but only when complexed with CT and acetyl-CoA. The fact that the BCCP-BC complex is only active in the presence of CT and acetyl-CoA is important for the regulation of enzyme activity because it means that ATP will only be hydrolyzed when acetyl-CoA is present. This is a classic example of substrate synergism in which the wasteful hydrolysis of ATP is prevented unless all the substrates are present. The structure reported here provides a structural context for understanding why the BCCP-BC complex is inactive in that the loop containing Lys122 to which biotin is attached is far away from the active site of biotin carboxylase. How the activity of the BCCP-BC complex is increased in the presence of CT and acetyl-CoA will have to await the structure of holo-acetyl-CoA carboxylase.

The fact that the hairpin loop is exposed to the solvent is also consistent with the observation that it is not biotinylated. Lys122 in BCCP is biotinylated by biotin protein ligase and therefore must be readily accessible in vivo. A superposition of the structure of *Pyrococcus horikoshii* biotin protein ligase

Table 1. Data Collection and Refinement Statistics for BCCP-BC Structures

Data Collection		
Space group	*C*2	$P2_1$
Cell dimensions		
a, *b*, *c* (Å)	233.0, 96.4, 120.6	100.6, 200.7, 121.3
β (°)	120.2	104.1
Resolution (Å)	2.49	3.74
R_{sym} [a,b]	6.2 (33.1)	19.2 (65.9)
$I / \sigma I$	11.2 (2.4)	7.2 (2.6)
Completeness (%)	98.5 (93.7)	98.3 (92.4)
Redundancy	2.5 (2.5)	4.3 (4.0)
Refinement		
Resolution (Å)	104.3-2.49	
Number of reflections	79,181	
R_{work} / R_{free} [c]	19.50/22.91	
Number of atoms	16,162	
Protein	15,643	
Ligand/ion	64	
Water	455	
B-factors		
Protein	39	
Ligand/ion	34	
Water	26	
rmsd		
Bond lengths (Å)	0.003	
Bond angles (°)	0.72	

[a]Values in parentheses are for the highest-resolution shell.
[b]$R_{sym} = (\Sigma|I_i - < I_i >| / \Sigma|I_i|)*100$, where I_i is the intensity of the i^{th} observation and $< I_i >$ is the mean intensity of the reflection.
[c]$R = (\Sigma||F_o| - |F_c||/ \Sigma|F_o|)*100$, where F_o and F_c are the observed and calculated structure factor amplitudes, respectively. R_{free} is calculated using 5% of reflections omitted from the refinement.

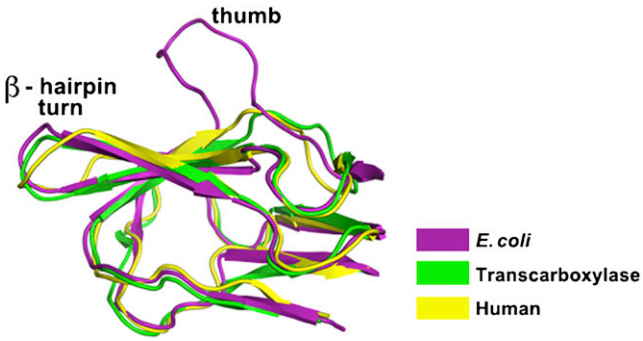

Figure 3. Superposition of BCCP
Superposition of *E. coli* BCCP from the BCCP-BC complex (purple) with the BCCP domain from human acetyl-CoA carboxylase (yellow) and the 1.3S subunit of transcarboxylase (green). The β-hairpin turns can be seen pointing to the left and the thumb of the *E. coli* BCCP is "thumbs up" toward the top of the figure.

complexed with BCCP (Bagautdinov et al., 2008) with the *E. coli* BCCP in the BCCP-BC complex shows the biotin protein ligase rests alongside BC with very little steric overlap (Figure S2). Thus, the structure of the BCCP-BC complex observed here is exactly what would be expected if the BCCP is not biotinylated.

BC Structure

The structure of the BC component in the BCCP-BC complex is virtually identical to previously determined structures of the BC homodimer (Chou et al., 2009; Mochalkin et al., 2008; Thoden et al., 2000; Waldrop et al., 1994). A superposition of the BC homodimer with one of the BC homodimers in the complex yielded a rmsd of 0.76 Å. BC is a member of the ATP-grasp superfamily of enzymes that all have a similar tertiary structure composed of three domains: N-terminal, C-terminal, and B-domain (Figure 2D) (Galperin and Koonin, 1997). The N- and C-terminal domains form the main body of the BC monomer while the B-domain either extends away from the other domains in the absence of ATP or rotates 45° to cover the active site in the presence of ATP (Thoden et al., 2000). In the BCCP-BC complex the B-domain is splayed open and therefore consistent with no substrates being bound.

Although the BCCP-BC complex described here did not contain any substrates, there was electron density in each BC active site that could be represented as an anion the size of phosphate or sulfate. Phosphate anions have been observed in structures of homodimeric BC (Thoden et al., 2000; Waldrop et al., 1994); however, sulfate ions were modeled in the BCCP-BC complex due to the high concentration of ammonium sulfate in the crystallization solution.

Structure of the Protein-Protein Interfaces

BCCP-BC Interfaces

BCCP binds to BC via two different interfaces. In the first interface, BCCP binds to the N-terminal domain of BC. The amino acids involved are located at the C terminus of strands β2 and β3 in BC and a loop connecting two β strands in BCCP (Figures 4A and 4B). One interaction involves the carbonyl oxygen of Cys50 from BC forming a hydrogen bond with the peptidic NH of Phe148 of BCCP, while in a second interaction the peptidic NH of Cys50 hydrogen bonds to the carboxylate group of Glu147 from BCCP. In addition, the side chains of His32 and Thr48 from BC interact with the carboxylate group of Glu147 from BCCP via a water molecule. Consistent with Glu147 being involved in binding to BC is that mutation of Glu147 to Lys (Chapman-Smith et al., 1999) in the domain comprising the C-terminal 87 residues of BCCP, which does exhibit activity with BC (Blanchard et al., 1999a), resulted in over a 100-fold increase in the K_m (unpublished data).

In the second interface the opposite end of the BCCP molecule interacts with residues in the N- and C-terminal domains of BC located in the opposite half of the BC tetramer (Figures 4A and 4C). Residues involved in this interface stem from the β1 strand of BCCP and the BC residues 56 and 57 located in a loop along with amino acids in the turn between two β strands. Specifically, the carboxylate of Asp149 of BCCP forms a hydrogen bond with the hydroxyl group of Tyr380 from BC (Figure 4C). The rest of the interactions at this interface are mediated through a putative sulfate ion and a water molecule (Figure 4C).

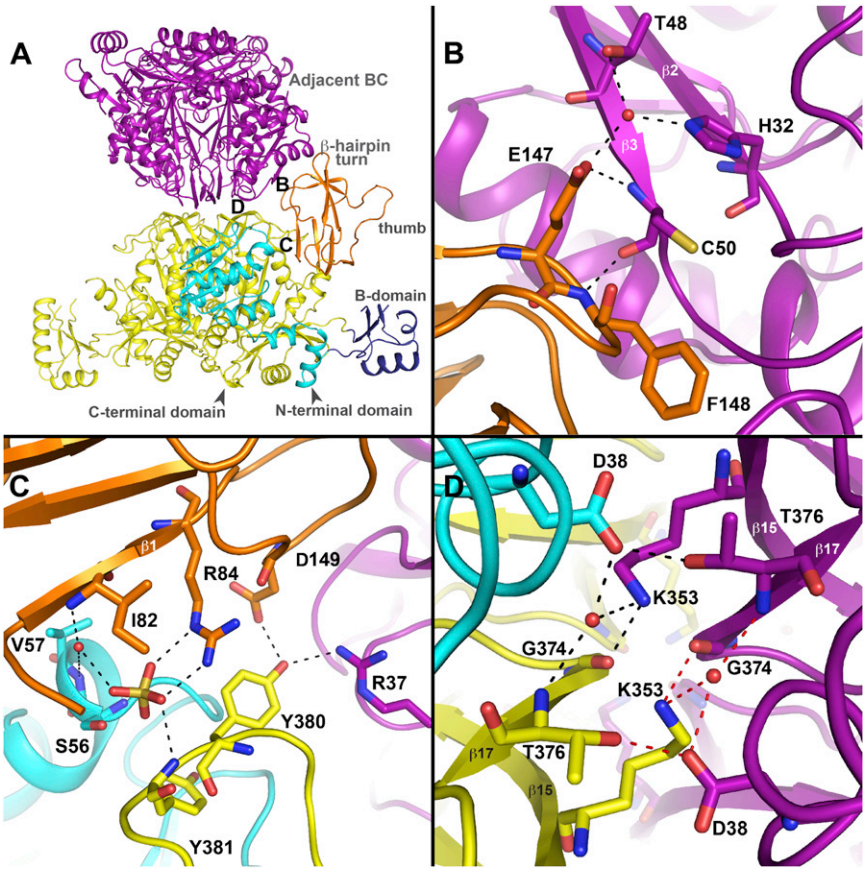

Figure 4. The BCCP-BC Complex Interfaces

Oxygen, nitrogen, sulfur atoms, and water are depicted in red, blue, gold, and red spheres, respectively. Residues are indicated by their single-letter abbreviation followed by their residue number in *E. coli*. Dashed lines depict hydrogen bonds and fall within 2.41 to 3.25 Å. The color scheme remains constant throughout the figure.

(A) BC homodimers are shown in purple (top) and yellow (bottom) of the complex. The N-terminal domain, B-domain, and C-terminal domain of one monomer of the yellow homodimer are labeled and colored light blue, dark blue, and yellow, respectively. One of the BCCPs binding these two homodimers together is shown in orange with the β-hairpin turn pointing to the purple homodimer. (A)–(D) correspond to the area that is enlarged in (B), (C), and (D), respectively. (B and C) A magnified view of the two BCCP-BC interfaces. (D) A magnified view of the BC-BC interface.

The presumed sulfate ion likely replaced a phosphate group, which was the case observed in the active site of BC described above. The residues in BC involved in this interaction are the side chain of Ser56 and the peptidic NH group of Tyr381, whereas in BCCP the interacting groups were the side chain of Arg84 and the peptidic NH group of Ile82. It is important to note that the BCCP-BC complex was stable to gel filtration chromatography in a buffer not containing sulfate and with a molecular weight consistent with a multimeric quaternary structure (Figure S1A).

The interactions observed in the *E. coli* BCCP-BC complex are similar to those observed for other biotin-dependent carboxylases in which structural information about the interaction of BCCP with either BC or CT is available (Fan et al., 2012; Huang et al., 2010, 2012; Lietzan et al., 2011; St Maurice et al., 2007; Xiang and Tong, 2008). The interfaces between BCCP and BC or CT in other biotin-dependent carboxylases were small and composed mostly of hydrogen and ionic bonds. Moreover, the residues involved in the protein-protein interactions were not conserved. The explanation given for the relatively weak BCCP-BC interface interactions was that BCCP has to undergo a large translocation between the BC and CT active sites. If the interface interactions were strong, indicative of hydrophobic interactions, then this would create a thermodynamic well preventing or slowing the ability of BCCP to translocate to the CT binding site. In fact, proteins that associate in a transient or non-obligatory manner show a general trend of interaction through hydrogen and ionic bonds instead of hydrophobic contacts (Nooren and Thornton, 2003; Ozbabacan et al., 2011).

The similarities of the BCCP-BC interfaces between *E. coli* and other biotin-dependent carboxylases are striking. The individual interfaces in the *E. coli* BCCP-BC complex are small, with buried surface areas of 240 Å^2 for the interface with the putative sulfate ion and 480 Å^2 for the other. However, these two small interfaces are repeated four times in the complex, giving a total buried surface area of 2,880 Å^2. Both interfaces are composed of hydrogen bonds and ionic interactions with no hydrophobic contacts. Moreover, the interface residues are not strictly conserved across a spectrum of Gram-positive and Gram-negative bacteria with the only exceptions being Cys50 and Tyr381 in BC and Glu147 in BCCP (Table S1).

Although the interfaces in the *E. coli* BCCP-BC complex are apparently strong enough to keep the complex intact on a gel filtration column, the small buried surface area for an individual BCCP molecule and the lack of hydrophobic interactions likely provide the appropriate amount of flexibility for movement of BCCP between the BC and CT active sites. Exactly how BCCP moves between the BC and CT active sites is not known. It might involve translocation of the entire BCCP as proposed in pyruvate carboxylase (St Maurice et al., 2007; Xiang and Tong, 2008), propionyl-CoA carboxylase (Huang et al., 2010), and methylcrotonyl-CoA carboxylase (Huang et al., 2012), which is consistent with the lack of hydrophobic residues because any partial dissociation of BCCP would not expose any hydrophobic residues to solvent.

BC-BC Interface

The BCCP-BC complex is also stabilized by a BC-BC interface. The buried surface area for the interface is small, 350 Å^2, suggesting a weak interaction; however, there are two identical BC-BC interfaces, which effectively doubles the interaction energy (Figures 4A and 4D). In fact, if the total buried surface

area for the two BC-BC interfaces (700 Å^2) is combined with the total buried surface area for the BCCP-BC interfaces, then the total buried surface area for the complex is 3,580 Å^2, which is consistent with the BCCP-BC complex being a permanent or obligate protein-protein interaction (Ozbabacan et al., 2011). Although the dissociation constant between BC and BCCP has not been determined, this level of total buried surface area suggests that it would be $<10^{-6}$ M (Ozbabacan et al., 2011).

The interacting residues are located in the C-domain of the BC monomer in β strands 15 and 17, with the exception of Asp38, which is in the N-terminal domain of BC. The residues that form the interface are duplicated such that there is two-fold symmetrical relationship for the interactions at each interface (Figure 4D). The two most prominent interactions are between the carbonyl oxygen of the strictly conserved Gly374 (Table S1) and the side chain of Lys353 and a hydrogen bond between the side chains of Thr376 and Asp38 (Figure 4D).

Comparison to BCCP-BC Structures from Other Biotin-Dependent Enzymes

While the structure presented here is the leading model of the BCCP-BC complex for acetyl-CoA carboxylase, the structure of BCCP and BC has been determined for related biotin-dependent carboxylases such as pyruvate carboxylase (Lietzan et al., 2011; St Maurice et al., 2007; Yu et al., 2009), propionyl-CoA carboxylase (Huang et al., 2010), methylcrotonyl-CoA carboxylase (Huang et al., 2012), and urea carboxylase (Fan et al., 2012). What distinguishes these enzymes from bacterial acetyl-CoA carboxylase is that the BC, BCCP, and CT functionalities are either all part of a single polypeptide chain or the BCCP and BC domains are located on the same polypeptide.

The only holoenzyme structure that shows an interaction between the BC and BCCP domains is the structure of pyruvate carboxylase from *Rhizobium etli* (Lietzan et al., 2011; St Maurice et al., 2007). The interaction in the C-domain between BC and BCCP in *R. etli* pyruvate carboxylase is not the same C-domain interaction observed in the *E. coli* BCCP-BC complex (Figure 5A). The reason for this difference becomes obvious in Figure 5B, which shows that in pyruvate carboxylase from *R. etli* there is a loop comprising residues Val52-Gly63 that protrudes from the main body of the protein at exactly the spot that the bacterial BCCP would bind to BC. Thus, the *E. coli* BCCP-BC complex described above does not have any similarities to BCCP-BC interactions observed in other biotin-dependent carboxylases. The apparent uniqueness of the bacterial BCCP-BC interaction is likely to be a consequence of not being covalently linked like the structures of similar biotin-dependent enzymes and, therefore, BCCP must be tethered to BC through noncovalent interactions. The differences observed here, however, do not preclude the possibility that the way BCCP interacts with the active site of BC is similar to pyruvate carboxylase (Lietzan et al., 2011).

Implications for Antibacterial Development

The dramatic increase in the number of pathogenic bacteria with extensive resistance to antibiotics has been well documented (Nathan, 2012; Spížek et al., 2010). Thus, there is a pressing need for new targets and biotin carboxylase has been validated as a novel target for antibacterial development (Miller et al., 2009; Mochalkin et al., 2009). Given that the protein-protein interface in *E. coli* BCCP-BC appears to be unique and presumably required for enzymatic activity, this greatly expands the number of potential target sites beyond just the traditional active sites.

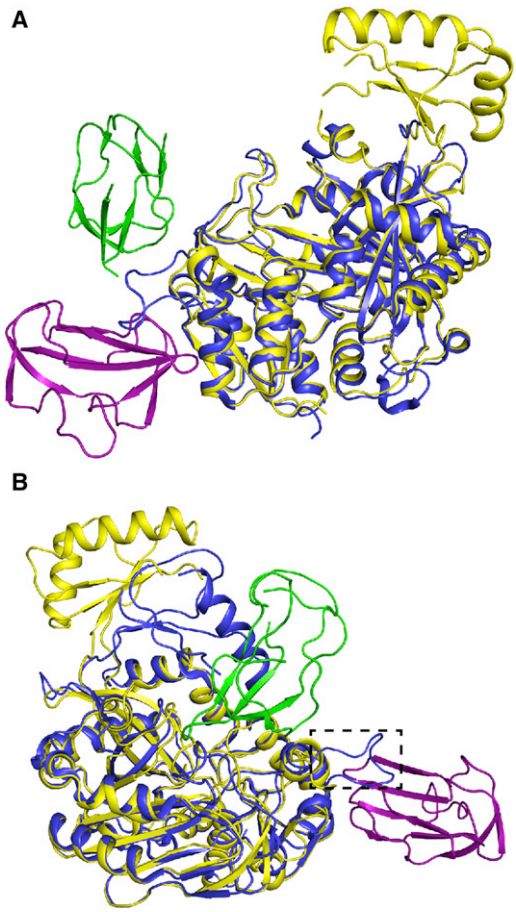

Figure 5. Biotin Carboxylase from *E. coli* Superimposed onto the Biotin Carboxylase Domain of *R. etli* Pyruvate Carboxylase

The BCCP-BC complex is shown in purple and gold, respectively, and the BCCP and BC domains of *R. etli* pyruvate carboxylase are shown in blue and green.

(A) Overlay of BC from *E. coli* with the BC domain from *R. etli* pyruvate carboxylase (Protein Data Bank ID 2F9Y).

(B) Overlay of BC from *E. coli* with the BC domain from *R. etli* pyruvate carboxylase (Protein Data Bank ID 3TW6). The dashed box indicates the loop in *R. etli* pyruvate carboxylase that would hinder *E. coli* BCCP binding.

EXPERIMENTAL PROCEDURES

Reagents, vector construction, protein expression and purification, and programs used to calculate rmsds and accessible surface areas are described in Supplemental Experimental Procedures.

Crystallization

Crystals were obtained by sitting drop vapor diffusion at room temperature using a 10 mg/ml solution of the BCCP-BC complex. The crystallization condition contained a reservoir solution of 0.2 M ammonium sulfate, 0.1 M BIS-TRIS (pH 6.5), and 25% w/v PEG 3350. The sitting drop contained a well to protein ratio of 1.75:2 μl. Crystals appeared after 3 months and were cryoprotected with a 30% v/v ethylene glycol/reservoir solution and then mixing that solution with crystal mother liquor in a 1:1 ratio. The crystal was submerged in the cryoprotectant and then immediately flash-cooled in liquid nitrogen.

X-Ray Data Collection, Structure Determination, and Refinement

X-ray diffraction data were collected to 2.49 Å at the Advanced Photon Source beamline NE-CAT 24-ID-E equipped with the ADSC Q315r detector. The data were processed and scaled using XDS (Kabsch, 2010). The crystal belonged to the C2 space group and had unit cell parameters a = 233.0 Å, b = 96.4 Å, c = 120.6 Å, and β = 120.2°. The asymmetric unit contained two BC homodimers and each monomer of BC was in complex with one BCCP molecule. The phase information was obtained by molecular replacement using Phaser (Adams et al., 2010) and a BCCP-BC heterodimer search model that was acquired from the solution of a 3.7 Å data set of a different crystal form (Table 1; Supplemental Experimental Procedures). The molecular replacement solution was further refined using several cycles of phenix.refine (Adams et al., 2010) and manual rebuilding in COOT (Emsley and Cowtan, 2004). All water molecules and ions added were manually verified after the final refinement. The final model consists of residues 1–163 and 167–446 for BC molecule A; 77–156 for BCCP molecule B; 1–161, 170–182, and 196–446 for BC molecule C; 79–156 for BCCP molecule D; 1–159, 170–183, and 197–446 for BC molecule E; 1–160, 169–184, and 196–446 for BC molecule F; 80–156 for BCCP molecule G; 80–156 for BCCP molecule I; and 455 water molecules. Twelve sulfate ions and one ethylene glycol molecule were included in the final model based on the shape of the difference electron density, composition of the crystallization and cryoprotectant solutions, and the refined B-factors. Data collection statistics are shown in Table 1.

ACCESSION NUMBERS

The atomic coordinates and structure factors for the BCCP-BC crystal structure have been deposited in the Protein Data Bank under accession number 4HR7.

SUPPLEMENTAL INFORMATION

Supplemental Information includes three figures, one table, and Supplemental Experimental Procedures and can be found with this article online at http://dx.doi.org/10.1016/j.str.2013.02.001.

ACKNOWLEDGMENTS

This work was funded in part by the National Science Foundation (MCB-0841134). Work conducted at the Advanced Photon Source on the Northeastern Collaborative Access Team beamlines is supported by the National Institutes of Health (5P41RR015301-10 and 8 P41 GM103403-10). Use of the Advanced Photon Source, an Office of Science User Facility operated for the U.S. Department of Energy (DOE) Office of Science by Argonne National Laboratory, was supported by the U.S. DOE under contract no. DE-AC02-06CH11357. We would like to thank Dr. Marcia Newcomer for her critical reading of the manuscript and Ashley Broussard for her expertise in figure design.

Received: November 2, 2012
Revised: February 1, 2013
Accepted: February 3, 2013
Published: March 14, 2013

REFERENCES

Adams, P.D., Afonine, P.V., Bunkóczi, G., Chen, V.B., Davis, I.W., Echols, N., Headd, J.J., Hung, L.W., Kapral, G.J., Grosse-Kunstleve, R.W., et al. (2010). PHENIX: a comprehensive Python-based system for macromolecular structure solution. Acta Crystallogr. D Biol. Crystallogr. *66*, 213–221.

Alves, J., Westling, L., Peters, E.C., Harris, J.L., and Trauger, J.W. (2011). Cloning, expression, and enzymatic activity of Acinetobacter baumannii and Klebsiella pneumoniae acetyl-coenzyme A carboxylases. Anal. Biochem. *417*, 103–111.

Athappilly, F.K., and Hendrickson, W.A. (1995). Structure of the biotinyl domain of acetyl-coenzyme A carboxylase determined by MAD phasing. Structure *3*, 1407–1419.

Bagautdinov, B., Matsuura, Y., Bagautdinova, S., and Kunishima, N. (2008). Protein biotinylation visualized by a complex structure of biotin protein ligase with a substrate. J. Biol. Chem. *283*, 14739–14750.

Bilder, P., Lightle, S., Bainbridge, G., Ohren, J., Finzel, B., Sun, F., Holley, S., Al-Kassim, L., Spessard, C., Melnick, M., et al. (2006). The structure of the carboxyltransferase component of acetyl-coA carboxylase reveals a zinc-binding motif unique to the bacterial enzyme. Biochemistry *45*, 1712–1722.

Blanchard, C.Z., and Waldrop, G.L. (1998). Overexpression and kinetic characterization of the carboxyltransferase component of acetyl-CoA carboxylase. J. Biol. Chem. *273*, 19140–19145.

Blanchard, C.Z., Chapman-Smith, A., Wallace, J.C., and Waldrop, G.L. (1999a). The biotin domain peptide from the biotin carboxyl carrier protein of Escherichia coli acetyl-CoA carboxylase causes a marked increase in the catalytic efficiency of biotin carboxylase and carboxyltransferase relative to free biotin. J. Biol. Chem. *274*, 31767–31769.

Blanchard, C.Z., Lee, Y.M., Frantom, P.A., and Waldrop, G.L. (1999b). Mutations at four active site residues of biotin carboxylase abolish substrate-induced synergism by biotin. Biochemistry *38*, 3393–3400.

Carey, P.R., Sönnichsen, F.D., and Yee, V.C. (2004). Transcarboxylase: one of nature's early nanomachines. IUBMB Life *56*, 575–583.

Chapman-Smith, A., Morris, T.W., Wallace, J.C., and Cronan, J.E., Jr. (1999). Molecular recognition in a post-translational modification of exceptional specificity. Mutants of the biotinylated domain of acetyl-CoA carboxylase defective in recognition by biotin protein ligase. J. Biol. Chem. *274*, 1449–1457.

Choi-Rhee, E., and Cronan, J.E. (2003). The biotin carboxylase-biotin carboxyl carrier protein complex of Escherichia coli acetyl-CoA carboxylase. J. Biol. Chem. *278*, 30806–30812.

Chou, C.Y., Yu, L.P., and Tong, L. (2009). Crystal structure of biotin carboxylase in complex with substrates and implications for its catalytic mechanism. J. Biol. Chem. *284*, 11690–11697.

Cronan, J.E., Jr. (2001). The biotinyl domain of Escherichia coli acetyl-CoA carboxylase. Evidence that the "thumb" structure id essential and that the domain functions as a dimer. J. Biol. Chem. *276*, 37355–37364.

Cronan, J.E., Jr., and Waldrop, G.L. (2002). Multi-subunit acetyl-CoA carboxylases. Prog. Lipid Res. *41*, 407–435.

Emsley, P., and Cowtan, K. (2004). Coot: model-building tools for molecular graphics. Acta Crystallogr. D Biol. Crystallogr. *60*, 2126–2132.

Fan, C., Chou, C.Y., Tong, L., and Xiang, S. (2012). Crystal structure of urea carboxylase provides insights into the carboxyltransfer reaction. J. Biol. Chem. *287*, 9389–9398.

Galperin, M.Y., and Koonin, E.V. (1997). A diverse superfamily of enzymes with ATP-dependent carboxylate-amine/thiol ligase activity. Protein Sci. *6*, 2639–2643.

Guchhait, R.B., Polakis, S.E., Dimroth, P., Stoll, E., Moss, J., and Lane, M.D. (1974). Acetyl coenzyme A carboxylase system of Escherichia coli. Purification and properties of the biotin carboxylase, carboxyltransferase, and carboxyl carrier protein components. J. Biol. Chem. *249*, 6633–6645.

Huang, C.S., Ge, P., Zhou, Z.H., and Tong, L. (2012). An unanticipated architecture of the 750-kDa α6β6 holoenzyme of 3-methylcrotonyl-CoA carboxylase. Nature *481*, 219–223.

Huang, C.S., Sadre-Bazzaz, K., Shen, Y., Deng, B., Zhou, Z.H., and Tong, L. (2010). Crystal structure of the alpha(6)beta(6) holoenzyme of propionyl-coenzyme A carboxylase. Nature *466*, 1001–1005.

James, E.S., and Cronan, J.E. (2004). Expression of two Escherichia coli acetyl-CoA carboxylase subunits is autoregulated. J. Biol. Chem. *279*, 2520–2527.

Kabsch, W. (2010). Xds. Acta Crystallogr. D Biol. Crystallogr. *66*, 125–132.

Lee, C.K., Cheong, H.K., Ryu, K.S., Lee, J.I., Lee, W., Jeon, Y.H., and Cheong, C. (2008). Biotinoyl domain of human acetyl-CoA carboxylase: Structural insights into the carboxyl transfer mechanism. Proteins *72*, 613–624.

Li, S.J., and Cronan, J.E., Jr. (1992a). The gene encoding the biotin carboxylase subunit of Escherichia coli acetyl-CoA carboxylase. J. Biol. Chem. *267*, 855–863.

Li, S.J., and Cronan, J.E., Jr. (1992b). The genes encoding the two carboxyltransferase subunits of Escherichia coli acetyl-CoA carboxylase. J. Biol. Chem. *267*, 16841–16847.

Lietzan, A.D., Menefee, A.L., Zeczycki, T.N., Kumar, S., Attwood, P.V., Wallace, J.C., Cleland, W.W., and St Maurice, M. (2011). Interaction between the biotin carboxyl carrier domain and the biotin carboxylase domain in pyruvate carboxylase from Rhizobium etli. Biochemistry *50*, 9708–9723.

Miller, J.R., Dunham, S., Mochalkin, I., Banotai, C., Bowman, M., Buist, S., Dunkle, B., Hanna, D., Harwood, H.J., Huband, M.D., et al. (2009). A class of selective antibacterials derived from a protein kinase inhibitor pharmacophore. Proc. Natl. Acad. Sci. USA *106*, 1737–1742.

Mochalkin, I., Miller, J.R., Evdokimov, A., Lightle, S., Yan, C., Stover, C.K., and Waldrop, G.L. (2008). Structural evidence for substrate-induced synergism and half-sites reactivity in biotin carboxylase. Protein Sci. *17*, 1706–1718.

Mochalkin, I., Miller, J.R., Narasimhan, L., Thanabal, V., Erdman, P., Cox, P.B., Prasad, J.V., Lightle, S., Huband, M.D., and Stover, C.K. (2009). Discovery of antibacterial biotin carboxylase inhibitors by virtual screening and fragment-based approaches. ACS Chem. Biol. *4*, 473–483.

Nathan, C. (2012). Fresh approaches to anti-infective therapies. Sci. Transl. Med. *4*, 140sr2.

Nenortas, E., and Beckett, D. (1996). Purification and characterization of intact and truncated forms of the Escherichia coli biotin carboxyl carrier subunit of acetyl-CoA carboxylase. J. Biol. Chem. *271*, 7559–7567.

Nooren, I.M., and Thornton, J.M. (2003). Diversity of protein-protein interactions. EMBO J. *22*, 3486–3492.

Ozbabacan, S.E., Engin, H.B., Gursoy, A., and Keskin, O. (2011). Transient protein-protein interactions. Protein Eng. Des. Sel. *24*, 635–648.

Reddy, D.V., Rothemund, S., Shenoy, B.C., Carey, P.R., and Sönnichsen, F.D. (1998). Structural characterization of the entire 1.3S subunit of transcarboxylase from Propionibacterium shermanii. Protein Sci. *7*, 2156–2163.

Sloane, V., and Waldrop, G.L. (2004). Kinetic characterization of mutations found in propionic acidemia and methylcrotonylglycinuria: evidence for cooperativity in biotin carboxylase. J. Biol. Chem. *279*, 15772–15778.

Soriano, A., Radice, A.D., Herbitter, A.H., Langsdorf, E.F., Stafford, J.M., Chan, S., Wang, S., Liu, Y.H., and Black, T.A. (2006). Escherichia coli acetyl-coenzyme A carboxylase: characterization and development of a high-throughput assay. Anal. Biochem. *349*, 268–276.

Spížek, J., Novotná, J., Rezanka, T., and Demain, A.L. (2010). Do we need new antibiotics? The search for new targets and new compounds. J. Ind. Microbiol. Biotechnol. *37*, 1241–1248.

St Maurice, M., Reinhardt, L., Surinya, K.H., Attwood, P.V., Wallace, J.C., Cleland, W.W., and Rayment, I. (2007). Domain architecture of pyruvate carboxylase, a biotin-dependent multifunctional enzyme. Science *317*, 1076–1079.

Thoden, J.B., Blanchard, C.Z., Holden, H.M., and Waldrop, G.L. (2000). Movement of the biotin carboxylase B-domain as a result of ATP binding. J. Biol. Chem. *275*, 16183–16190.

Waldrop, G.L., Rayment, I., and Holden, H.M. (1994). Three-dimensional structure of the biotin carboxylase subunit of acetyl-CoA carboxylase. Biochemistry *33*, 10249–10256.

Xiang, S., and Tong, L. (2008). Crystal structures of human and Staphylococcus aureus pyruvate carboxylase and molecular insights into the carboxyltransfer reaction. Nat. Struct. Mol. Biol. *15*, 295–302.

Yao, X., Wei, D., Soden, C., Jr., Summers, M.F., and Beckett, D. (1997). Structure of the carboxy-terminal fragment of the apo-biotin carboxyl carrier subunit of Escherichia coli acetyl-CoA carboxylase. Biochemistry *36*, 15089–15100.

Yu, L.P., Xiang, S., Lasso, G., Gil, D., Valle, M., and Tong, L. (2009). A symmetrical tetramer for S. aureus pyruvate carboxylase in complex with coenzyme A. Structure *17*, 823–832.